CellPress

Joule

Perspective

Historical market projections and the future of silicon solar cells

Bruno Vicari Stefani,[1,*] Moonyong Kim,[2] Yuchao Zhang,[2] Brett Hallam,[2,3] Martin A. Green,[2] Ruy S. Bonilla,[4] Christopher Fell,[1] Gregory J. Wilson,[1,5] and Matthew Wright[4]

SUMMARY

The International Technology Roadmap for Photovoltaics (ITRPV) is a globally recognized annual report discussing and projecting photovoltaic (PV) industry trends. Over the past decade, the silicon PV manufacturing landscape has undergone several rapid changes. By analyzing ITRPV reports from 2012 to 2023, we highlight some key discrepancies between projected industry trends and estimated actual market share. Some technologies have vastly exceeded the expected trends, e.g., the passivated emitter and rear cell and the use of gallium as the dominant p-type dopant. However, other projections have not occurred as quickly as expected, e.g., adopting silicon heterojunction cells and shifting to n-type wafers. In this work, we provide insights into the fidelity of projected trends by discussing some of the factors causing such rapid technological changes. By reflecting on 10 years of roadmap data, we highlight the fast-moving nature of the PV industry, meaning that business-as-usual projections must be assessed with caution.

INTRODUCTION

The International Technology Roadmap for Photovoltaics (ITRPV) annual reports highlight developments and trends in the photovoltaic (PV) market and are considered a guide for the crystalline silicon PV industry.[1] The ITRPV reports are published by a group of international experts from across the entire PV supply chain. The data in the reports are gathered via questionnaires sent to individuals and companies operating in all sectors of the PV industry up to the creation of the PV module. These include polysilicon, wafers, cells, modules, and PV manufacturing equipment. In this article, we analyze the historical ITRPV predictions for silicon solar cell technologies and silicon wafer types. The analysis presented here is based on the following: (1) silicon wafer crystalline structure, (2) silicon solar cell technology, (3) silicon wafer polarity, and (4) p-type silicon dopant element. For each category, the market share projections from ITRPV reports spanning 2012 to 2023 are analyzed.[1–13] Compiling historical data allows the ITRPV market projections to be compared with annual market share estimates issued since 2012, which permits assessment of the accuracy of such projections. Furthermore, a decade of market projections provided a means to identify trends in such projections for different technologies over time. We examine the underlying technological factors contributing to the observed trends and discrepancies in market projections for silicon wafers and cell technologies. Based on our observations, we discuss the potential impact of recent technological advances on the future composition of the silicon PV market.

SILICON WAFER CRYSTAL STRUCTURE

The silicon wafers used in solar cell manufacturing can have different crystal structures based on the crystal growth technique employed. The first mainstream

CONTEXT & SCALE

Over the past decade, a revolution has occurred in the manufacturing of crystalline silicon solar cells. The conventional "Al-BSF" technology, which was the mainstream technology for many years, was replaced by the "PERC" technology. These technological advancements have significantly impacted electricity generation globally, with total solar photovoltaic installations surpassing 1 TW last year.

The International Technology Roadmap for Photovoltaics (ITRPV) has published reports tracking technological changes in silicon solar cell manufacturing over the years. Here, we analyze ITRPV's silicon wafer and solar cell market projections published between 2012 and 2023. Analyzing historical market projections revealed discrepancies when comparing projected industry trends with estimated market shares for different technologies. In this perspective, we examine these discrepancies and discuss the underlying factors driving such rapid technological changes.

commercial silicon solar cells (based on the aluminum back surface field [Al-BSF] technology) were manufactured with both monocrystalline and multicrystalline silicon wafers. Multicrystalline wafers are cut from solid ingots formed by directionally solidifying molten silicon. Due to the lack of a seed crystal to define the growth, the resulting wafers contain many crystals of different orientations, which leads to more crystallographic defects. In contrast, monocrystalline wafers are typically fabricated using the Czochralski (Cz) method, where a seed crystal with a particular crystal orientation is dipped into molten silicon, held by a pulling rod. As the seed is slowly removed from the molten silicon and rotated, an ingot is formed with a crystal orientation matching that of the seed. Consequently, monocrystalline silicon wafers exhibit lower concentrations of impurities and crystallographic defects than multicrystalline material. However, larger concentrations of interstitial oxygen are introduced in monocrystalline wafers during wafer growth using the Cz method.[14] Due to the high concentrations of oxygen and boron (the latter was commonly used as p-type dopant), monocrystalline wafers were affected by a metastable defect which caused light (more precisely carrier)-induced degradation (LID), known as boron-oxygen (BO) LID (hence, BO-LID).[15,16] BO-LID was initially reported to reduce the conversion efficiency of passivated emitter and rear cell (PERC) and p-type silicon heterojunction (SHJ) solar cells by 3.5%$_{rel}$[17] and 14.3%$_{rel}$,[18] respectively.

In 2012, multicrystalline silicon wafers represented over 60% of the solar cell market. The dominance of multicrystalline wafers during that period was related to the lower processing costs associated with directional solidification,[19] lower susceptibility to BO-LID,[20] and higher packing factor of square wafers in solar modules.[21] Hence, the use of multicrystalline silicon increased between 2012 and 2015. The predicted (future) and estimated actual market shares for monocrystalline and directionally solidified silicon wafers as reported in successive ITRPV roadmaps are displayed in Figure 1. In the figure, monocrystalline silicon includes Cz, magnetic Cz, and float-zone silicon wafers. However, Cz wafers represent over 99% of the monocrystalline silicon market. Directionally solidified silicon includes traditional multicrystalline, high-performance multicrystalline, and mono-like (also known as cast- and quasi-mono) silicon wafers. For a comprehensive discussion on crystalline silicon wafer types and processing approaches, see the excellent review by Ballif et al.[22]

Figure 1 indicates a consistent underestimate by the PV industry participants of the extent to which monocrystalline silicon would overtake directionally solidified silicon as the preferred wafering technology. When PERC solar cells were first commercialized, p-type multicrystalline silicon wafers still dominated the solar cell market. The transition in cell design (from Al-BSF to PERC) was accompanied by the introduction of additional hydrogen in the wafer's bulk. The additional hydrogen originates from the rear dielectric passivation layers and diffuses into the wafers during fast firing.[23] This additional hydrogen facilitates the passivation of BO defects (in monocrystalline silicon),[24] electronically active defects introduced by transition metal impurities (e.g., interstitial iron),[25] and crystallographic defects (particularly present in multicrystalline silicon).[26] However, the additional hydrogen incorporated in the wafers during PERC manufacturing introduced a then novel degradation mechanism, referred to as light- and elevated temperature-induced degradation (LETID).[27,28] LETID was initially reported to reduce the conversion efficiency of PERC solar cells by up to 16%$_{rel}$.[29] Despite all silicon wafers being susceptible to LETID, the negative impact of the defect was found to be more severe in p-type multicrystalline silicon wafers.[30,31] During that period, practical solutions for BO-LID were developed,[32–34] and the cost of monocrystalline silicon wafers decreased due to improvements in ingot growth and processing throughput by manufacturers (including the introduction

[1]CSIRO Energy, Newcastle Energy Centre, Mayfield West, Newcastle, NSW 2304, Australia

[2]School of Photovoltaic and Renewable Energy Engineering, The University of New South Wales, Kensington, NSW 2052, Australia

[3]ITP Renewables, Turner, ACT 2612, Australia

[4]Department of Materials, University of Oxford, Oxford OX1 3PH, UK

[5]School of Engineering, University of Newcastle, Callaghan, NSW 2308, Australia

*Correspondence: vsbruno@proton.me

https://doi.org/10.1016/j.joule.2023.11.006

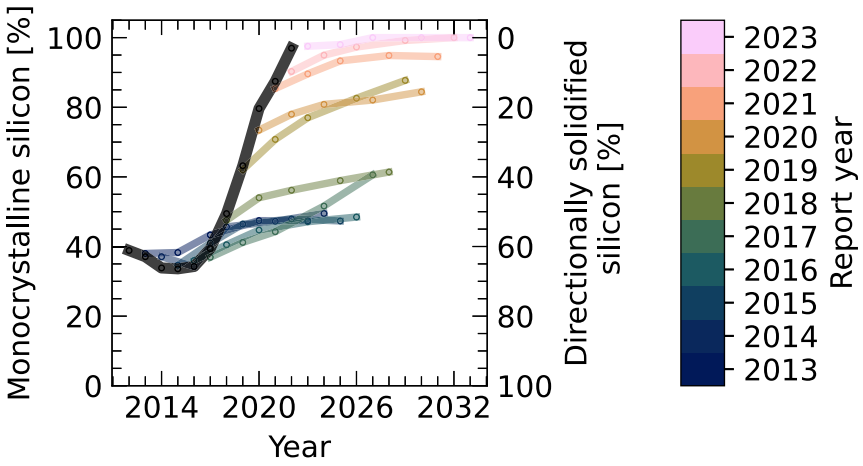

Figure 1. Silicon wafer crystal structure market projections

Market share projections (color markers) for monocrystalline and directionally solidified silicon wafers were extracted from the International Technology Roadmap for Photovoltaics (ITRPV) annual reports. The black markers represent the estimated actual market share of the year prior to each report. The overlap between black and color markers indicates an accurate prediction. The lines serve as a guide to the eye. Monocrystalline silicon includes Cz, magnetic Cz, and float-zone silicon wafers. Directionally solidified silicon includes traditional multicrystalline, high-performance multicrystalline, and mono-like wafers.

of diamond wire sawing).[35] Additionally, passivating both emitter and rear provided a pathway to fully utilize the high-lifetime (low recombination) potential of monocrystalline wafers. Combined with LETID concerns in p-type multicrystalline silicon, these factors contributed to a fast transition toward monocrystalline silicon wafers from 2018. The short-term predictions for monocrystalline and directionally solidified silicon wafer usage agreed well with the estimated actual market shares until 2018, after which the trends rapidly changed in favor of monocrystalline silicon. The market share of directionally solidified silicon wafers was approximately 3% in 2022, despite predictions of 2022 market shares of 10%–45%. This highlights that the industry shifted toward monocrystalline silicon much faster and to a broader monocrystalline silicon usage than predicted.

SOLAR CELL ARCHITECTURE

The main silicon solar cell technologies can be grouped into six categories: (1) Al-BSF, (2) PERC, (3) tunnel oxide passivating contact/polysilicon on oxide (TOPCon/POLO) where TOPCon is the name most adopted for the technology, (4) SHJ, (5) interdigitated back contact (IBC), which includes metal-wrap-through designs, and (6) tandem solar cells. A schematic diagram of each cell design is depicted in Figure 2. Note the schematics illustrate the overall characteristics of each cell design, and design variations might be observed in commercial products. Commercial tandem solar cells are not illustrated as the architecture of the first product to enter the market is still to be determined. Recent progress by OxfordPV, with a conversion efficiency of 28.6% for a commercial-sized (258.15 cm^2) tandem solar cell, suggests that a two-terminal perovskite on SHJ solar cell might be the first commercial tandem.[36]

The first mainstream commercial silicon solar cells were based on the Al-BSF cell design. Al-BSF solar cells are named after the BSF formed during the fast-firing step required for contact formation. The conversion efficiency of Al-BSF is severely limited

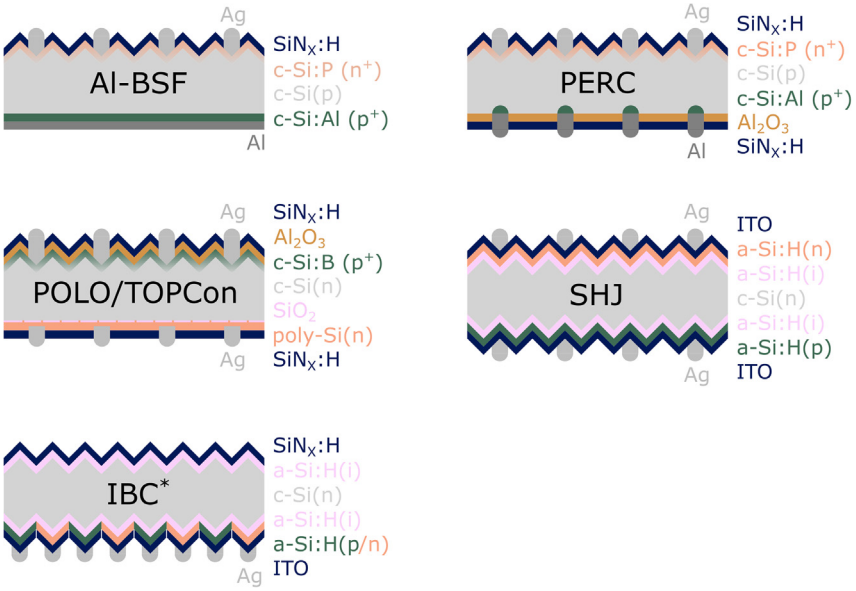

Figure 2. Overview of silicon solar cell architectures

Schematic illustration of different single-junction silicon cell architectures. *The IBC structure is presented based on a SHJ contacting scheme; however, multiple different approaches are possible.

by recombination losses at the full area silicon to metal rear contact. The PERC design, which features localized silicon-to-metal contacts, provided a cost-effective alternative to Al-BSF in mass production environments,[37] with better performance due to much lower rear surface recombination. The significant gain in performance, combined with inherent similarities in cell designs, meant that the transition to PERC was favorable. Essentially, two additional processing steps (rear passivation and local opening of rear contacts) are required to transition from Al-BSF to PERC.[37] The benefits associated with the transition are illustrated in the record conversion efficiency of each cell design. The record PERC solar cell fabricated in 1999 exhibited a conversion efficiency of 25.0%,[38] whereas the record Al-BSF solar cell fabricated in 2017 had a conversion efficiency of 20.3%.[39] For these reasons, the market share of Al-BSF solar cells rapidly decreased over the ensuing years, whereas the market share of PERC solar cells rapidly increased post-2015.

Figure 4 displays the market share predictions and estimates of actual share for silicon solar cell technologies based on the ITRPV annual reports. The plot highlights that predictions for Al-BSF and PERC solar cells were in reasonable agreement with estimated actual market shares in the short term. However, the long-term predictions for PERC were underestimated, as the market share of other technologies (e.g., SHJ, IBC, and tandems) was predicted to rapidly increase. The reports issued between 2013 and 2020 estimated that the predicted adoption of other cell technologies would limit the market share of PERC to approximately 40%–70%. However, although the market share of Al-BSF rapidly decreased from 75% to 10% between 2018 and 2021, the market share of PERC increased from 35% to more than 80%. Several technical factors can help explain the rapid transition from Al-BSF to PERC. First, a technological breakthrough occurred with the development of a thin aluminum oxide passivating layer for the rear p-type silicon, which was soon transferred from research to an industrial scale. Second, equipment manufacturers quickly developed high-throughput tools for the additional processing steps,

enabling the new cell design to be implemented without significant disruptive changes to the cell processing know-how.[40] Meanwhile, the cost of solar modules decreased substantially, making improvements in cell efficiency a substantial contributor to reductions in the levelized cost of electricity. Thus, manufacturers established brand-new PERC manufacturing lines with new tools (featuring a much higher throughput) and a cleaner production environment, enabling the technology's full potential. These factors led to a rapid decommissioning of Al-BSF production. The rapid decommissioning of Al-BSF technology was well captured in the first China Photovoltaic Industry Association (CPIA) Development Roadmap from 2016, where projections indicated a market share of ≈10% by 2022 for the technology.[41] The report also projected a rapid uptake of PERC and its variants, for which market share would surpass 75% by 2022.[41] In contrast, the market projections on the 2017 ITPRV report (2016 data) indicated that Al-BSF would still retain a market share >10% in 2027, with a much slower PERC uptake reaching ≈65% in 2027. The comparison of market share projections issued by the 2016 CPIA and 2017 ITRPV is depicted in Figure S1.

The practical conversion efficiency limit of PERC solar cells in mass production environments is estimated to be approximately 24%.[42] Trina Solar has already reported a conversion efficiency of 24.5% for a full area > 441 cm^2 industrial PERC solar cell.[43] This suggests that a new cell technology with greater efficiency potential will be required if the industry is to maintain the constant ≈0.5%$_{abs}$/year historical growth in cell efficiency.[17,40] Cell technologies featuring passivating contacts have the potential to enable conversion efficiencies above 26% in mass production environments. In such devices, a thin passivation layer is inserted between the silicon wafer and metal cell contacts, minimizing recombination losses at the contact interface.[44] Currently, two commercial solar cell technologies feature passivating contacts in their design, namely TOPCon/POLO and SHJ. Conversion efficiencies of 26.4% and 26.8% were recently demonstrated for large-area TOPCon[45] and SHJ[46] solar cells, respectively. The broad commercial adoption of both technologies is discussed next.

The market share of TOPCon solar cells has been rapidly increasing since they were first introduced. This is assisted by similarities between the TOPCon and PERC technologies,[35,40,47] which have similar cell designs, processes, and production equipment. The ITRPV predictions for the TOPCon solar cell market closely match the estimated actual market shares for the technology so far. This suggests that the rapid growth in TOPCon market share might be maintained, potentially approaching 60% within a decade. However, the transition from PERC to TOPCon might be even faster, like the transition from Al-BSF to PERC. This rapid transition is illustrated in recent announcements by leading manufacturers. JinkoSolar shipped 17.8 GW of solar modules in the second quarter of 2023, of which 10.4 GW (≈58%) were n-type modules.[48] Although total module shipments increased by 36.2% compared with the previous quarter, n-type module shipments increased by 74.1%.[48] Trina Solar cell capacity is forecast to reach 75 GW by the end of 2023, with 40 GW based on n-type TOPCon cells.[49]

Al-BSF, PERC, and TOPCon technologies share many similarities, namely diffused emitters, high-temperature metallization (well above 600°C), and surface dielectric passivation layers. These features, however, are not shared with SHJ technology, where the emitter, BSF, and passivation layers are formed via deposition of thin amorphous (or nano-/micro-crystalline) silicon or silicon-rich thin films, and the metallization is realized at approximately 200°C.[50] The excellent surface passivation

provided by such films enables high V_{OC} values (>750 mV reported),[51] which in turn enable high conversion efficiencies (well above 25%). The current world record conversion efficiency of 26.8% for a single-junction silicon solar cell based on n-type SHJ technology clearly illustrates its potential.[52] However, this promise has not yet translated into wide commercial adoption. This is highlighted by the large discrepancy between the predictions outlined in the ITRPV reports and the actual market share estimations for SHJ. We also note a similar discrepancy between the predictions outlined in the CPIA reports and the actual market estimations for SHJ. Despite the current small market share of SHJ being accurately captured in the 2016 CPIA report, the 2019 edition predicted a similar growth rate to the ITRPV (see Figure S2). The 2022 CPIA report, however, predicts a more aggressive growth for SHJ technology. According to the report, SHJ solar cells will approach a market share of 20% by 2025 before passing the 30% mark in 2030 (see Figure S3).[53]

Several factors contribute to the slow adoption of SHJ technology. The first is related to the higher capital expenditure (CapEx) of SHJ technology, which, according to the CPIA, was 360 million RMB/GW for SHJ in 2022.[53] In the same period, the CapEx of TOPCon and PERC were 190 and 150 million RMB/GW, respectively.[53] Although turnkey solutions with a guaranteed efficiency level can reduce the entry requirements for new players, this does not lead to significant reductions in equipment cost. The second barrier to the uptake of SHJ technology relates to module efficiency, which is currently at the same level (≈22.5%) for leading SHJ and TOPCon products.[54] The lack of significant module efficiency gains over TOPCon makes it hard to justify new investment in SHJ, given the higher investment in equipment required. The third relates to sustainability concerns over the use of indium and larger amounts of silver in SHJ solar cells. Enormous progress has been made recently in the development of low-indium (e.g., aluminum-doped zinc oxide / indium tin oxide stacks)[55,56] SHJ solar cells in research and development (R&D), and some manufacturers are now implementing measures to reduce indium usage in mass production.[57] However, further work is required to reduce indium concentrations to a level that could support multi-terawatt production.[58] Similarly, there has been significant progress in the development of silver-lean[51] and silver-free[59,60] SHJ solar cells, and the wide adoption of such technologies by industry could contribute to the uptake of SHJ in the future. A fourth barrier to the uptake of SHJ technology is the limited number of players. However, several companies have made the move from p-type technology to SHJ. These include but are not limited to the following: Risen, Jinergy, Akcome, REC, URECO, and Canadian Solar, where the latter two are transitioning from PERC to both TOPCon and SHJ.[54] The last barrier to the uptake of SHJ technology is their dependence on n-type wafers, which, for a given thickness are about 6% more expensive than p-type wafers.[61] However, SHJ technology uses much thinner wafers than PERC, which contributes to reducing the wafer cost in SHJ manufacturing. This relates to the low-temperature fabrication sequence and symmetrical structure of SHJ solar cells. The low-temperature manufacturing enables the use of thinner wafers without incurring additional yield losses associated with traditional high-temperature processing routes (e.g., PERC and TOPCon). Thus, some wafer manufacturers now offer 110-μm-thick n-type wafers for SHJ manufacturing at a lower price than 150-μm-thick p-type wafers for PERC manufacturing.[62] However, switching to p-type at the same thickness could bring costs down even further.

Here, it is important to note that the current record conversion efficiencies for both n- and p-type single-junction silicon solar cells were achieved using SHJ technology. The conversion efficiency of the record p-type SHJ solar cell is approximately $0.2\%_{abs}$ lower than its n-type counterpart.[52] Work from Chang et al. indicates that

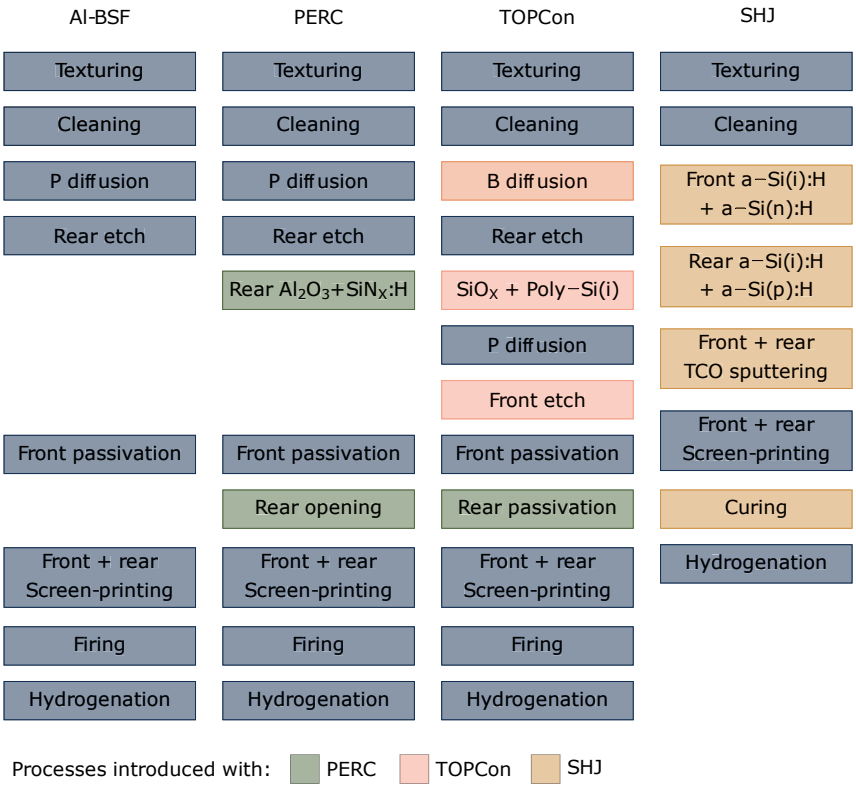

Figure 3. Silicon solar cell fabrication sequences

Fabrication sequences for Al-BSF, PERC, TOPCon, and SHJ solar cells. This schematic illustrates the overall similarities and differences in cell processing across silicon solar cell technologies. The blue boxes indicated processes in common with Al-BSF technology. The green and pink boxes indicate the additional processes required by PERC and TOPCon, respectively. The orange boxes indicate processes exclusive to SHJ. We note that variations in cell processing by different manufacturers occur.

for this efficiency gap and a n-type wafer cost premium of 8%, replacing n- by p-type silicon wafers might be cost-effective for SHJ technology.[63] However, the potential advantage of switching to p-type wafers in SHJ technology becomes less attractive as the cost premium between n- and p-type wafers diminishes. Challenges to replacing n- by p-type wafers in SHJ technology include minimizing the concentration of interstitial iron in the as-grown wafers, which even in concentrations as low as 10^9 cm^{-3} can pose significant limitations to carrier lifetime in cell concepts where surface recombination is minimized.[64]

To illustrate the key difference in cell processing used in manufacturing, the overall processing sequences for Al-BSF, PERC, TOPCon, and SHJ are depicted in Figure 3. We note that variations in cell processing/materials occur for different manufacturers; however, the processing sequences in Figure 3 highlight the key processes used in each technology. For a detailed cell processing overview, see the excellent review article by Ballif et al.[22] Here, it is possible to visualize the incremental steps required to move from Al-BSF to PERC and finally to TOPCon. These similarities in cell processing enabled the know-how developed over the years to be carried on through the technologies. The vastly different processing of SHJ solar cells might help explain their relatively slow adoption. The same applies to IBC technology. The sequence for IBC solar cells is not illustrated here due to the many possible approaches for cell fabrication, which can be achieved via homojunction, high-temperature passivating contacts, or SHJ approaches.

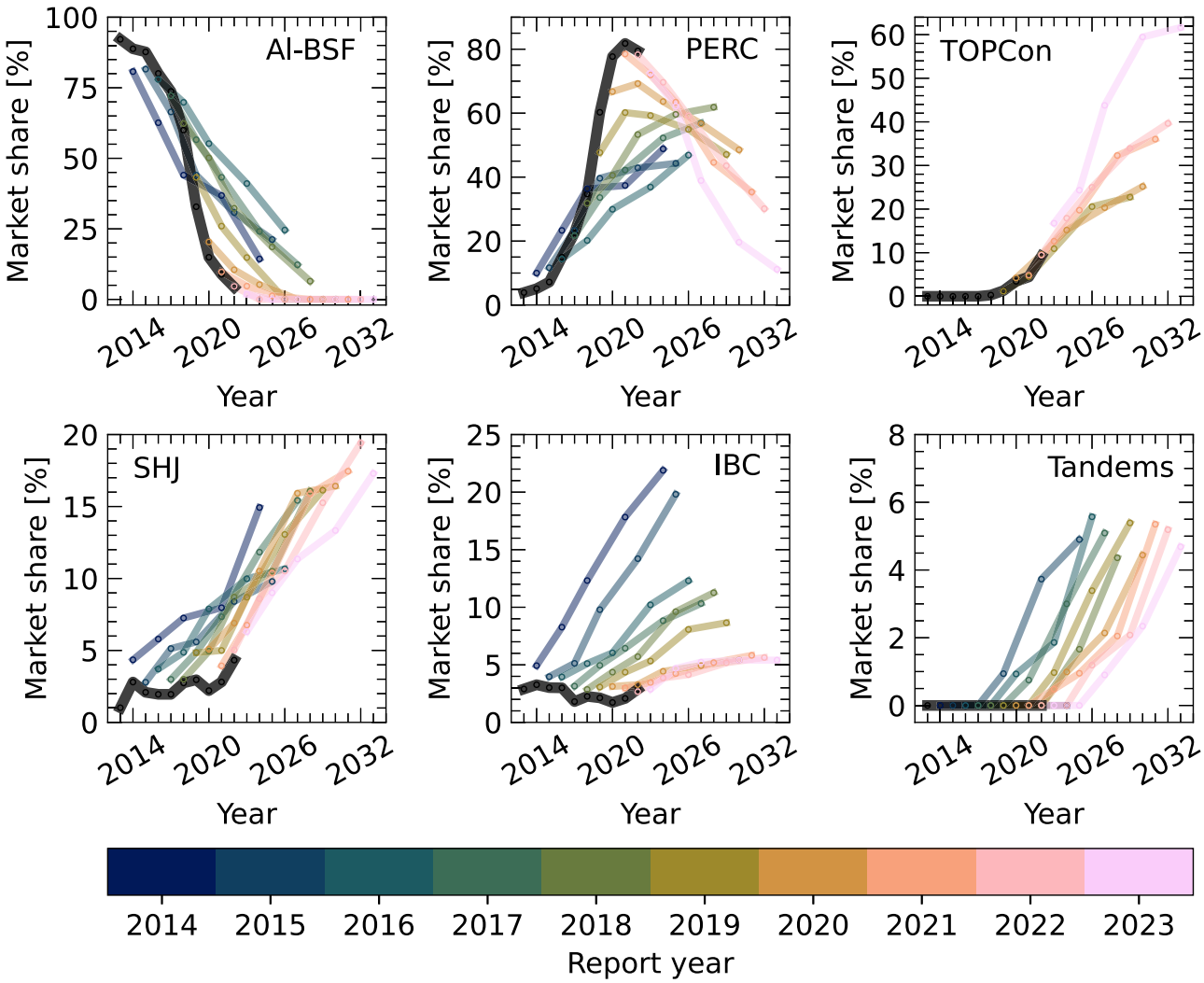

Figure 4. Silicon solar cell architecture market projections

Market share projections (color markers) for silicon solar cell technologies based on the International Technology Roadmap for Photovoltaics (ITRPV) annual reports. The black markers represent the estimated actual market share of the year prior to each report. The overlap between black and color markers indicates an accurate prediction. The lines serve as a guide to the eye.

The common feature between all approaches is the use of masking to form the interdigitated back contacts.

The adoption of IBC cell technology has been less rapid than anticipated. However, recent product launches by LONGi Solar, Aiko, and Maxeon indicate that this trend may soon change. Although some p-type PERC manufacturers are shifting toward SHJ technology, other manufacturers, like LONGi Solar and Aiko, have started offering IBC modules. LONGi Solar reported module conversion efficiencies of up to 23.2% using their hybrid-passivated back contact (HPBC) design, which combines p-type silicon wafers with an IBC cell structure.[65] This illustrates the potential of applying p-type silicon wafers to industrial solar cells featuring passivating contacts (interdigitated on the back side). Aiko Solar reported a maximum mass production module conversion efficiency of 24% for their n-type all-back contact (ABC) technology, based on n-type silicon wafers and a silver-free IBC structure.[66] Maxeon recently reported a commercial IBC module conversion efficiency of 23% for their

Maxeon 6 technology, drawing on the expertise of over 20 years of manufacturing by SunPower.[67]

Finally, we note that silicon tandem solar cells are yet to gain a share in the market, lagging well behind earlier expectations. The leading tandem product architecture is still to be determined. A promising candidate is perovskite-on-silicon tandem solar cells in two- or four-terminal configurations, although lack of the required stability remains a major obstacle for perovskite-based PV.[68] If perovskite materials are required for the first tandem PV product to reach the market, then the most recent ITRPV predictions may well be optimistic in suggesting growth from 2025. Most markets directly or indirectly require PV modules to have passed the ≈50 stress tests specified in the two relevant International Electrotechnical Comission (IEC) standards (IEC 61215 for quality and IEC 61730 for safety—note: soon to be amalgamated into a larger IEC 61730). Even if/when laboratory testing shows the technology can pass these tests, there are still at least two barriers to formal qualification: (1) metastability in perovskite cells affects the reproducibility of performance measurements,[69] making it difficult to discern the effects of stress testing definitively, and (2) these standards contain stabilization requirements that are defined specifically for the recognized PV material technology types, and no such definitions are included for perovskites yet. However, Babics et al. recently reported encouraging results on the outdoor stability of perovskite-on-silicon monolithic tandem solar cells.[70] The cells were formed by depositing a p-i-n perovskite on top of a SHJ bottom cell, which is the configuration used in record perovskite-on-silicon tandems with conversion efficiencies exceeding 30%.[71–73] In their study, encapsulated cells retained over 80% of their initial power outdoors in harsh environmental conditions after one complete calendar year. However, the stability of such devices still needs to match that of commercial silicon modules, where some manufacturers provide guaranteed power outputs greater than 88% of the module's initial power after 40 years of operation.[74]

SILICON WAFER POLARITY

In silicon PV, crystalline silicon wafers are doped with group III (e.g., boron or gallium) or group V (e.g., phosphorus) atoms to increase their conductivity and provide the base side of the p-n junction. Doping crystalline silicon with group V atoms increases the number of available free electrons, and the resulting material is referred to as n-type silicon. Conversely, doping crystalline silicon with group III atoms creates an excess of free holes, thus producing p-type silicon. When the first commercial silicon solar cells were developed, p-type doping was preferred over n-type doping. This was related to the superior stability of p-type silicon during irradiation studies for space applications,[75] which were the first commercial applications for silicon solar cells. Later, the terrestrial silicon PV industry was developed drawing on the expertise from early space PV industry. Thus, the first commercial silicon solar cells for terrestrial applications were based on p-type silicon wafers, which also benefited from the manufacturing advantages of phosphorus-doped emitters, uniformly doped ingots (B segregation coefficient), and higher electron minority carrier mobility. However, commercially available n-type wafers normally offer a higher minority carrier lifetime than p-type wafers of the same resistivity. This is related to the greater sensitivity of p-type silicon wafers to common metal point defects such as interstitial iron and the susceptibility of boron-doped (B-doped) Cz-grown silicon to BO-LID.[76]

The quality of the bulk wafer becomes more critical to cell performance once other recombination mechanisms (e.g., surface-related) are minimized. Once research

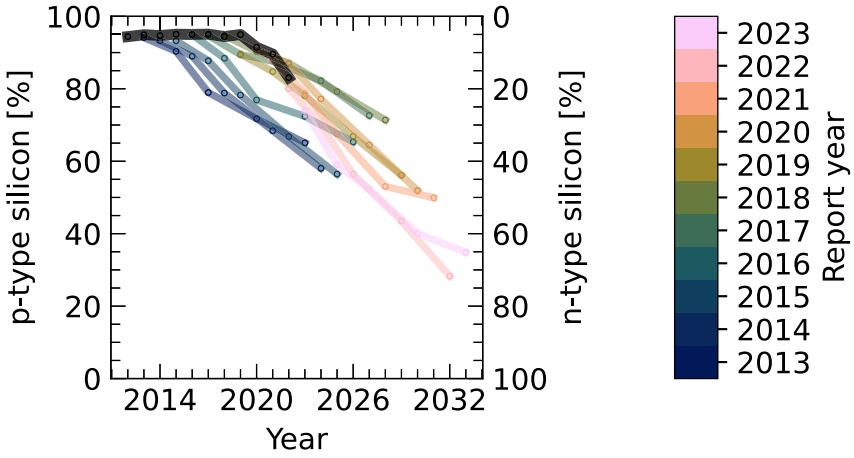

Figure 5. Silicon wafer polarity market projections

Market share projections (color markers) for silicon wafer type (polarity) extracted from the International Technology Roadmap for Photovoltaics (ITRPV) annual reports. The black markers represent the estimated actual market share of the year prior to each report. The overlap between black and color markers indicates an accurate prediction. The lines serve as a guide to the eye.

for terrestrial PV applications began, and through the early days of industrial manufacturing, n-type monocrystalline wafers doped with phosphorus were the wafer of choice for high-efficiency stable solar cells, due to their inherent immunity to BO-LID. These wafers are about 6% more expensive than their p-type counterparts of identical thickness.[61] The main factors contributing to the higher cost of n-type wafers are their still limited market share,[77] the lower yield,[78] and the lower number of acceptable recharges during ingot growth[78] compared with p-type wafers. The lower yield and acceptable recharges are related to the inherent requirement of high carrier lifetime (i.e., low bulk recombination) wafers by SHJ and TOPCon architectures, where surface-related recombination is much lower than traditional p-type architectures.[79] The yield losses arise in variations in minority carrier lifetime and resistivity along an ingot, which relates to the segregation coefficient and accumulation of impurities present during crystal growth.[79] This creates an impurity-rich region in the tail end of Cz-grown ingots, which is unmarketable due to the strict lifetime requirements of n-type technologies.[78,79] Similarly, impurities can accumulate in the residual melt after each ingot growth.[80] Thus, the accumulation of impurities can negatively impact the carrier lifetime after each recharging/pulling cycle. This limits the number of ingots pulled from each crucible to maintain acceptable carrier lifetimes.

Due to the predicted rapid adoption of SHJ technology in the industry since 2014, the market share of n-type silicon was also predicted to rapidly increase (see Figure 5). The predicted increase in n-type silicon usage, however, was significantly overestimated, and it was pushed forward over the years in parallel with the predicted increased adoption of SHJ solar cells. Consequently, the n-type silicon market share remained stable at approximately 5% until 2018. During this period, the quality gap (e.g., minority carrier lifetime and stability) between p- and n-type silicon wafers resulted in a premium market for n-type-based solar cells. Despite SHJ solar cells (also traditionally based on n-type silicon)[81] being in the market since 1997,[82] it was actually the introduction of the TOPCon design that boosted n-type silicon adoption. The introduction of TOPCon technologies in the solar cell market led to an increase in the use of n-type silicon, approaching 17% in 2022. As discussed in the previous section, the market share of TOPCon solar cells is likely to rapidly

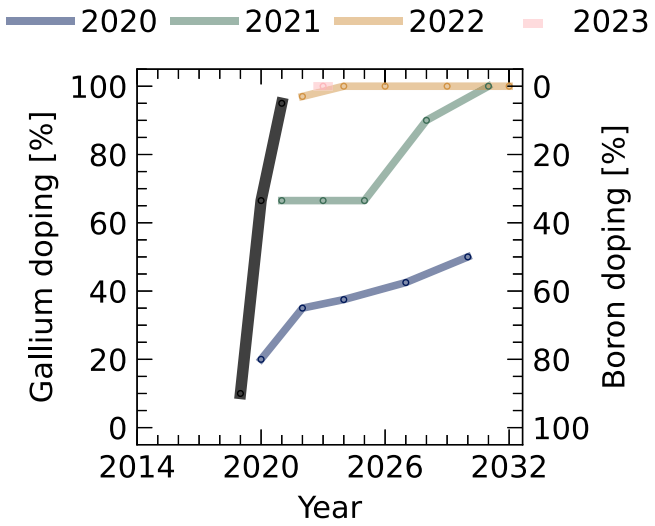

Figure 6. Dopant elements for p-type silicon market projections

Market share projections (color markers) for p-type silicon-doping agents extracted from the International Technology Roadmap for Photovoltaics (ITRPV) annual reports. The black markers represent the estimated actual market share of the year prior to each report. The overlap between black and color markers indicates an accurate prediction. The lines serve as a guide to the eye.

increase in the upcoming years. Consequently, the market share of n-type silicon wafers is also expected to increase. The market predictions issued in the last ITRPV reports indicate that n-type technologies will become the mainstream PV products sometime between 2026 and 2029. PV Tech research also suggests that n-type-based technologies will become the mainstream product by 2026, before completely replacing p-type-based technologies in 2030.[83] However, the adoption of n-type silicon, driven by the rapid adoption of TOPCon technology, might be even faster than predicted. This will contribute to reducing the cost of n-type silicon wafers, benefiting all n-type-based technologies.

DOPANT ELEMENTS FOR P-TYPE SILICON

One key difference between industrial PERC and TOPCon solar cells is the wafer type used. The main drawback of using commercial-grade p-type B-doped Cz-grown silicon wafers in TOPCon devices is their susceptibility to BO-LID. This could be avoided by switching to gallium as the doping element,[84] and this change has been widely adopted by wafer manufacturers since the patents blocking its use expired in 2020.[85] Figure 6 illustrates the rapid transition toward gallium as the dopant for p-type silicon in industry. The market share of gallium-doped (Ga-doped) wafers increased from approximately 10% in 2019 to over 95% in 2021. The latest ITRPV report indicates that boron as a dopant for p-type material disappears in 2023.[13] This rapid transition was enabled by the ease of replacing p-type B- by Ga-doped silicon wafers in PERC solar cells, where no modifications to the cell structure were required. Applying p-type Ga-doped wafers to TOPCon cells, for example, would likely require changes to the cell structure.

By modifying the TOPCon structure to accommodate a p-type silicon wafer, Richter et al. demonstrated a 26.0% p-type TOPCon solar cell, which performed better than n-type TOPCon solar cells (25.8%) fabricated in parallel.[86] A key aspect of the structure used by Richter et al. is the relocation of the p-n junction to the rear of the device. This takes advantage of the high lifetimes now observed in low-resistivity p-type silicon

wafers to realize the minority carrier lateral transport in the wafer's bulk. As a result, the opto-electrical requirements of the front surface layers (including emitter and dielectric films) can be relaxed, reducing parasitic absorption and recombination losses in these layers. For example, the hard-to-make lightly doped emitters (especially boron for an n-type wafer) are omitted with the rear-junction p-type TOPCon approach. This front surface emitter is currently a barrier to pushing TOPCon efficiencies higher in industrial manufacturing. The rear-junction approach was also adopted in n-type SHJ in the past and has become the standard SHJ solar cell design.[87] The additional lateral transport also provides an opportunity to increase finger spacing, which reduces shading losses. Another interesting aspect of the proposed p-type rear-junction TOPCon solar cell is the potential use of alloyed aluminum underneath the front contact, which avoids both the use of silver and front boron diffusion. These design and processing advantages combined with stability, high lifetimes, and lower cost of p-type wafer processing could directly impact the wide adoption of TOPCon solar cells and n-type silicon wafers by industry. Min et al. reported a conversion efficiency of 23.1% (and V_{OC} of 717 mV) for a full-area p-type rear-junction TOPCon solar cell using industry-compatible materials and processes.[88,89] These included a commercial-grade 0.8 Ω•cm p-type Ga-doped Cz-grown silicon wafer, alloyed aluminum front contacts, and fully screen-printed contacts. However, the efficiency of p-type TOPCon still needs to improve to be competitive with n-type TOPCon solar cells, which have already achieved an efficiency of 26.4%.[45] Challenges to further increase p-type TOPCon cell efficiency include but are not limited to the following: improving the lifetime of low-resistivity p-type wafers, preventing wafer contamination during cell processing and reducing recombination in the Al/silicon contacts.[90] Despite the inherent immunity of p-type Ga-doped silicon wafers to BO-LID (provided they are not co-doped with large concentrations of boron), instabilities in solar cells fabricated with such wafers have been reported.[64,91,92] However, this observed degradation is much less severe than for BO-LID. Understanding the defect(s) and mechanism(s) responsible for the observed degradation behaviors is a prerequisite for adopting p-type Ga-doped wafers in a new cell design. This also applies to modifications done to PERC solar cells, where degradation under carrier injection has been reported in some instances.[91] However, stable SHJ solar cells fabricated with commercially available p-type Ga-doped wafers commonly used in PERC solar cell manufacturing have already been demonstrated.[93,94]

Conclusions

In this perspective, we analyze the historical projections for silicon solar cells from the ITRPV reports and compare these with the corresponding estimated actual market shares. The scope of the analysis includes the silicon crystal structure, cell architecture, and dopant types. This analysis highlights some significant discrepancies between the historically projected market shares and the market shares that were eventually realized. The discrepancies come in two forms. First, the market share for some technologies transitioned much more rapidly than the projections. Examples of this include the adoption of PERC as the mainstream cell technology and the shift to gallium as the dominant p-type dopant. The reasons for these rapid transitions were very different, being a sudden improvement and availability for PERC manufacturing tools and the expiration of patents for gallium doping, respectively. These rapid transitions tell us that business-as-usual evolution does not always describe the reality of the fast-moving PV industry, and thus, projections for the future must be approached with some caution. The second kind of discrepancy is seen when some technologies projected to gain market share over time do not take off. Examples of this include the projected growth in market share for both SHJ cells and n-type wafers. In both cases, the lack of observed growth is linked to the rapid and sustained success of p-type PERC cells. We also note that despite

optimistic predictions of tandem products entering the market as early as 2019, the first commercial tandem product is still to be announced. Recent improvements in the conversion efficiency and stability of perovskite-on-silicon tandem solar cells indicate that such cells might be the first commercial tandem product. Looking into the future, the adoption of TOPCon technology is closely following the projections outlined in the ITRPV reports, which indicate a market share of 20% to 60% within the next decade. However, TOPCon technology might experience an even more rapid uptake, as occurred with PERC. This could see the growth in n-type wafer market share as previously projected. High-lifetime Ga-doped monocrystalline silicon wafers are now commercially available. These wafers might provide a cost-effective alternative to n-type silicon wafers in industrial solar cells featuring passivating contacts. However, further work is required to bring the efficiency of such devices to the same level as commercial n-type technologies.

SUPPLEMENTAL INFORMATION

Supplemental information can be found online at https://doi.org/10.1016/j.joule.2023.11.006.

ACKNOWLEDGMENTS

The authors thank Dr Pietro Altermatt for useful scientific discussions. B.V.S. acknowledges the CSIRO Research Office for his CERC fellowship. B.H. and M.K. would like to acknowledge the Australian Government through the support of the Australian Renewable Energy Agency (ARENA) funding of the ARENA 2022/TRAC010 project. R.S.B. was supported by the Royal Academy of Engineering under the Research Fellowship scheme (RF\201819\18\38). This work was supported by the UK Engineering and Physical Sciences Research Council grant number EP/V038605/1.

AUTHOR CONTRIBUTIONS

B.V.S. and M.K. conceptualized the work. B.V.S. developed the methodology, performed the formal analysis, investigation, data curation, visualization, and wrote the original draft. M.K., Y.Z., M.A.G., C.F., B.H., R.S.B., and M.W. reviewed and edited the manuscript. M.W. supervised the work. G.J.W. administered the project and acquired funding.

DECLARATION OF INTERESTS

The authors declare no competing interests.

REFERENCES

1. Fischer, M., Woodhouse, M.A., Herritsch, S., and Trube, J. (2022). International Technology Roadmap for Photovoltaic (ITRPV): Publication of the 13th Edition. https://www.vdma.org/viewer/-/v2article/render/50902381.

2. Fischer, M., Woodhouse, M.A., Herritsch, S., and Trube, J. (2021). International Technology Roadmap for Photovoltaic (VDMA).

3. Fischer, M., Woodhouse, M.A., Herritsch, S., and Trube, J. (2020). International Technology Roadmap for Photovoltaic (VDMA).

4. Sanderson, L., Templeton, T., Lorenz, A., Cellere, G., Wiedmann, S., Bernreuter, J., Hülsmann, P., Haase, J., Fischer, M., Arbitman, N., von Beulwitz, R., et al. (2019). International Technology Roadmap for Photovoltaic (ITRPV), 10th edition. https://pv-manufacturing.org/wp-content/uploads/2019/03/ITRPV-2019.pdf.

5. Pujari, N.S., Cellere, G., Falcon, T., Zwegers, M., Bernreuter, J., Haase, J., Coletti, G., Romijn, I., Kroon, J., Geerligs, B., et al. (2018). International Technology Roadmap for Photovoltaic, (ITRPV) 2017 results, 9th edition. http://www.pvmen.com/upload/attachment/201803/20/053037/ITRPV%20Ninth%20Edition%202018_1.pdf.

6. Metz, A., Fischer, M., and Trube, J. (2017). International Technology Roadmap for Photovoltaic 8th edition. Crystalline Silicon Technology–current status and outlook..

7. Cellere, G., Forstner, H., Falcon, T., Zwegers, M., Bernreuter, J., Xing, G., Haase, J., Jooss, W., Antoniadis, H., Coletti, G., et al. (2016). International Technology Roadmap for Photovoltaic (VDMA).

8. Metz, A., Demenik, G., Richter, A., Vlasenko, T., Buchovskaya, I., Zwegers, M., Xu, H., Luan, A., Wertz, R., Stassen, A., and Forstner, H. (2015). International Technology Roadmap for Photovoltaic (ITRPV) 2014 results (VDMA).

9. Forstner, H., Bandil, S., Zwegers, M., Bollen, R., Coletti, G., Sinke, W., Bultma, J., Wyers, P., Wertz, R., Wu, S., et al. (2014). International Technology Roadmap for Photovoltaic, 5th edition. https://www.semi.org/sites/semi.org/files/docs/ITRPV_2014_Roadmap_Revision1_140324.pdf.

10. Froitzheim, A., Suarez, F., Fischer, M., Spiess, T., Petter, K., Mohr, A., Gerlach, A., Jorg, M.,

Trager, M., Guo, A., et al. (2013). International Technology Roadmap for Photovoltaic, 4th Edition (VDMA e.V.).

11. Berger, M., Welsh, M., Fischer, M., Muller, J., Jrtschil, A., Spiess, T., Petter, K., Engelhart, P., Kusters, K.H., Metz, A., et al. (2012). International Technology Roadmap for Photovoltaics (VDMA e.V.).

12. Raithel, S., Metz, A., Solar, S., and Fischer, M. (2011). International Technology Roadmap for PV (VDMA).

13. Fischer, M., Woodhouse, M.A., Baliozian, P., and Trube, J. (2023). International Technology Roadmap for Photovoltaics (ITRPV): Publication of the 14th Edition. https://www.vdma.org/viewer/-/v2article/render/78984725.

14. Bothe, K., Sinton, R., and Schmidt, J. (2005). Fundamental boron-oxygen-related carrier lifetime limit in mono- and multicrystalline silicon. Prog. Photovolt.: Res. Appl. *13*, 287–296.

15. Niewelt, T., Schon, J., Warta, W., Glunz, S.W., and Schubert, M.C. (2017). Degradation of crystalline silicon due to boron–oxygen defects. IEEE J. Photovolt. *7*, 383–398.

16. Lindroos, J., and Savin, H. (2016). Review of light-induced degradation in crystalline silicon solar cells. Sol. Energy Mater. Sol. Cells *147*, 115–126.

17. Fertig, F., Lantzsch, R., Mohr, A., Schaper, M., Bartzsch, M., Wissen, D., Kersten, F., Mette, A., Peters, S., Eidner, A., et al. (2017). Mass production of p-type Cz silicon solar cells approaching average stable conversion efficiencies of 22 %. Energy Procedia *124*, 338–345.

18. Vicari Stefani, B., Soeriyadi, A., Wright, M., Chen, D., Kim, M., Zhang, Y., and Hallam, B. (2020). Large-area boron-doped 1.6 Ω cm p-type Czochralski silicon heterojunction solar cells with a stable open-circuit voltage of 736 mV and efficiency of 22.0%. Sol. RRL *4*, 2000134.

19. Möller, H.J., Funke, C., Rinio, M., and Scholz, S. (2005). Multicrystalline silicon for solar cells. Thin Solid Films *487*, 179–187.

20. Schultz, O., Glunz, S.W., Riepe, S., and Willeke, G.P. (2006). High-efficiency solar cells on phosphorus gettered multicrystalline silicon substrates. Prog. Photovolt.: Res. Appl. *14*, 711–719.

21. Saga, T. (2010). Advances in crystalline silicon solar cell technology for industrial mass production. NPG Asia Mater. *2*, 96–102.

22. Ballif, C., Haug, F.-J., Boccard, M., Verlinden, P.J., and Hahn, G. (2022). Status and perspectives of crystalline silicon photovoltaics in research and industry. Nat. Rev. Mater. *7*, 597–616.

23. Hallam, B., Chen, D., Kim, M., Stefani, B., Hoex, B., Abbott, M., and Wenham, S. (2017). The role of hydrogenation and gettering in enhancing the efficiency of next-generation Si solar cells: an industrial perspective. Physica Status Solidi (a) *214*, 1700305.

24. Hallam, B.J., Hamer, P.G., Ciesla née Wenham, A.M., Chan, C.E., Vicari Stefani, B., and Wenham, S. (2020). Development of advanced hydrogenation processes for silicon solar cells via an improved understanding of the behaviour of hydrogen in silicon. Prog. Photovolt.: Res. Appl. *28*, 1217–1238.

25. Liu, A., Sun, C., and Macdonald, D. (2014). Hydrogen passivation of interstitial iron in boron-doped multicrystalline silicon during annealing. J. Appl. Phys. *116*, 194902.

26. Sio, H.C., Phang, S.P., Fell, A., Wang, H., Zheng, P., Chen, D., Zhang, X., Zhang, T., Wang, Q., Jin, H., et al. (2019). The electrical properties of high performance multicrystalline silicon and mono-like silicon: material limitations and cell potential. Sol. Energy Mater. Sol. Cells *201*, 110059.

27. Chen, D., Vaqueiro Contreras, M., Ciesla, A., Hamer, P., Hallam, B., Abbott, M., and Chan, C. (2021). Progress in the understanding of light- and elevated temperature-induced degradation in silicon solar cells: a review. Prog. Photovolt.: Res. Appl. *29*, 1180–1201.

28. Ramspeck, K., et al. (2012). Light induced degradation of rear passivated mc-Si solar cells. In Proceedings of the 27th European Photovoltaic Solar Energy Conference and Exhibition, pp. 861–865.

29. Petter, K., Hübener, K., Kersten, F., Bartzsch, M., Fertig, F., and Müller, J. (2016). Dependence of LeTID on brick height for different wafer suppliers with several resistivities and dopants. Proceedings of the 9th Int. Work. Cryst. Silicon Sol. Cells. *6*, 1–17.

30. Chen, D., Kim, M., Stefani, B.V., Hallam, B.J., Abbott, M.D., Chan, C.E., Chen, R., Payne, D.N.R., Nampalli, N., Ciesla, A., et al. (2017). Evidence of an identical firing-activated carrier-induced defect in monocrystalline and multicrystalline silicon. Sol. Energy Mater. Sol. Cells *172*, 293–300.

31. Fertig, F., Krauß, K., and Rein, S. (2015). Light-induced degradation of PECVD aluminium oxide passivated silicon solar cells: light-induced degradation of PECVD aluminium oxide passivated silicon solar cells. Phys. Status Solidi RRL *9*, 41–46.

32. Herguth, A., and Hahn, G. (2013). Towards a high throughput solution for boron-oxygen related regeneration. In Proceedings of the 28th European Photovoltaic Solar Energy Conference and Exhibition, pp. 1507–1511.

33. Wilking, S., Engelhardt, J., Ebert, S., Beckh, C., Herguth, A., and Hahn, G. (2014). High speed regeneration of BO-defects: improving long-term solar cell performance within seconds. In 29th European Photovoltaic Solar Energy Conference and Exhibition (WIP), pp. 366–372.

34. Hamer, P., Hallam, B., Abbott, M., and Wenham, S. (2015). Accelerated formation of the boron-oxygen complex in p-type Czochralski silicon. Physica Rapid. Research. Ltrs. *9*, 297–300.

35. Wilson, G.M., Al-Jassim, M., Metzger, W.K., Glunz, S.W., Verlinden, P., Xiong, G., Mansfield, L.M., Stanbery, B.J., Zhu, K., Yan, Y., et al. (2020). The 2020 photovoltaic technologies roadmap. J. Phys. D: Appl. Phys. *53*, 493001.

36. OxfordPV. Oxford PV sets new solar cell world record. (2023). https://www.oxfordpv.com/news/oxford-pv-sets-new-solar-cell-world-record. (accessed 2023-06-01).

37. Green, M.A. (2015). The passivated emitter and rear cell (PERC): from conception to mass production. Sol. Energy Mater. Sol. Cells *143*, 190–197.

38. Green, M.A. (2009). The path to 25% silicon solar cell efficiency: history of silicon cell evolution. Prog. Photovolt.: Res. Appl. *17*, 183–189.

39. Kim, K.H., Park, C.S., Lee, J.D., Lim, J.Y., Yeon, J.M., Kim, I.H., Lee, E.J., and Cho, Y.H. (2017). Record high efficiency of screen-printed silicon aluminum back surface field solar cell: 20.29%. Jpn. J. Appl. Phys. *56*, 8MB25.

40. Chen, Y., Chen, D., Altermatt, P.P., Zhang, S., Wang, L., Zhang, X., Xu, J., Feng, Z., Shen, H., and Verlinden, P.J. (2022). Technology evolution of the photovoltaic industry: learning from history and recent progress. Published online September 30, 2023. Prog. Photovolt. 1–11.

41. Wang, S., Chen, J., Hua, J., Liu, Y., Wang, S., Zhu, B., and Jin, Y. (2016). China Photovoltaic Industry Development Roadmap 2016.

42. Zhang, Y., Wang, L., Chen, D., Kim, M., and Hallam, B. (2021). Pathway towards 24% efficiency for fully screen-printed passivated emitter and rear contact solar cells. J. Phys. D *54*, 214003.

43. Trina Solar. Trina Solar sets 24th World record with 24.5% efficient 210 PERC cell. (2022). https://www.trinasolar.com/us/resources/newsroom/210-perc-cell-sets-world-record-24.5%25-efficiency. (accessed 2023-03-06).

44. Allen, T.G., Bullock, J., Yang, X., Javey, A., and De Wolf, S. (2019). Passivating contacts for crystalline silicon solar cells. Nat. Energy *4*, 914–928.

45. JinkoSolar's high-efficiency N-type monocrystalline silicon solar cell sets our new record with maximum conversion efficiency of 26.4%. https://www.jinkosolar.com/en/site/newsdetail/1827. (accessed 2023-09-06)

46. Lin, H., Yang, M., Ru, X., Wang, G., Yin, S., Peng, F., Hong, C., Qu, M., Lu, J., Fang, L., et al. (2023). Silicon heterojunction solar cells with up to 26.81% efficiency achieved by electrically optimized nanocrystalline-silicon hole contact layers. Nat. Energy *8*, 789–799.

47. Yan, D., Cuevas, A., Michel, J.I., Zhang, C., Wan, Y., Zhang, X., and Bullock, J. (2021). Polysilicon passivated junctions: the next technology for silicon solar cells? Joule *5*, 811–828.

48. Norman W. JinkoSolar shipped 17.8GW of modules in Q2, continues n-type growth. PV Tech; (2023). https://www.pv-tech.org/jinkosolar-shipped-17-8gw-of-modules-in-q2-continues-n-type-growth/. (accessed 2023-09-06).

49. Trina Solar. Trina Solar's accumulated shipments of 210mm modules have surpassed 75GW, financial report for first half of 2023 shows. (2023). https://www.trinasolar.com/en-apac/resources/newsroom/aptrina-solar's-accumulated-shipments-210mm-modules-have-surpassed-75gw-financial. (accessed 2023-09-06).

50. De Wolf, S., Descoeudres, A., Holman, Z.C., and Ballif, C. (2012). High-efficiency silicon

heterojunction solar cells: a review. Green *2*, 7–24.

51. Razzaq, A., Allen, T.G., Liu, W., Liu, Z., and De Wolf, S. (2022). Silicon heterojunction solar cells: techno-economic assessment and opportunities. Joule *6*, 514–542.

52. Green, M.A., Dunlop, E.D., Siefer, G., Yoshita, M., Kopidakis, N., Bothe, K., and Hao, X. (2023). Solar cell efficiency tables (version 61). Prog. Photovolt. *31*, 3–16.

53. Wang, S., Hua, J., Li, J., Wang, Q., Zhang, T., Ling, L., Wang, X., Zhang, H., Wu, D., Bai, H., and Yang. (2022). J. China Photovoltaic Industry Development Roadmap, pp. 2022–2023.

54. Chunduri S. Monthly TaiyangNews update on commercially available high efficiency solar modules. Taiyang News; (2023). https://taiyangnews.info/top-modules/top-solar-modules-listing-august-2023/. (accessed 2023-08-28).

55. Tang, Q., Duan, W., Lambertz, A., Bittkau, K., Yaqin, M.A., Zhao, Y., Zhang, K., Yang, Q., Qiu, D., Gunkel, F., et al. (2023). > 85% indium reduction for high-efficiency silicon heterojunction solar cells with aluminum-doped zinc oxide contacts. Sol. Energy Mater. Sol. Cells *251*, 112120.

56. Gageot, T., Veirman, J., Jay, F., Muñoz-Rojas, D., Denis, C., Couderc, R., Ozanne, A., Monna, R., Zogbo, S., and Cabal, R. (2023). Feasibility test of drastic indium cut down in SHJ solar cells and modules using ultra-thin ITO layers. Sol. Energy Mater. Sol. Cells *261*, 112512.

57. Maxwell Technologies. Maxwell promotes lower costs for HJT cell manufacturing via three approaches to reduce use of indium. PV Tech; (2023). https://www.pv-tech.org/industry-updates/maxwell-promotes-lower-costs-for-hjt-cell-manufacturing-via-three-approaches-to-reduce-use-of-indium/. (accessed 2023-08-28).

58. Zhang, Y., Kim, M., Wang, L., Verlinden, P., and Hallam, B. (2021). Design considerations for multi-terawatt scale manufacturing of existing and future photovoltaic technologies: challenges and opportunities related to silver, indium and bismuth consumption. Energy Environ. Sci. *14*, 5587–5610.

59. Yu, C., Zou, Q., Wang, Q., Zhao, Y., Ran, X., Dong, G., Peng, C., Allen, V., Cao, X., Zhou, J., et al. (2023). Silicon solar cell with undoped tin oxide transparent electrode. Nat. Energy *8*, 1119–1125.

60. Carroll D. SunDrive achieves 26.41% efficiency with copper-based solar cell tech. PV Magazine; 2022. https://www.pv-magazine.com/2022/09/05/sundrive-achieves-26-41-efficiency-with-copper-based-solar-cell-tech/. (accessed 2023-09-07).

61. Chunduri S. Half wafer processing and thinner wafers becoming standard practice in HJT solar cell production, leading to increased efficiency and cost savings. Taiyang News; (2023). https://taiyangnews.info/technology/half-wafer-processing-for-hjt-modules/. (accessed 2023-09-07).

62. Taiyang News. Weekly overview on prices for polysilicon, wafers, cells, modules & solar glass. (2023). https://taiyangnews.info/price-index/taiyangnews-pv-price-index-cw35/. (accessed 2023-09-07).

63. Chang, N.L., Wright, M., Egan, R., and Hallam, B. (2020). The technical and economic viability of replacing n-type with p-type wafers for silicon heterojunction solar cells. Cell Rep. Phys. Sci. *1*.

64. Post, R., Niewelt, T., Kwapil, W., and Schubert, M. (2022). Carrier lifetime limitation of industrial Ga-doped Cz-grown silicon after different solar cell process flows. IEEE J. Photovolt. *12*, 238–243.

65. LONGi. The Hi-MO 6 series – stunning design and high efficiency exclusively dedicated to the DG market. (2023). https://www.longi.com/en/distributorbriefing/hi-mo6-intersolar-2023/. (accessed 2023-09-07).

66. Bhambhani, A. (2023). TÜV SÜD certifies Aiko Solar's claim for 24% efficiency for all back contact solar panels – a new world record for commercial modules. https://taiyangnews.info/technology/cracking-24-module-efficiency-level/.

67. Maxeon Solar Technologies. Maxeon Solar Technologies extends solar panel technology leadership position. (2023). https://mediaroom.maxeon.com/2023-06-01-Maxeon-Solar-Technologies-Extends-Solar-Panel-Technology-Leadership-Position. (accessed 2023-09-07).

68. Duan, L., Walter, D., Chang, N., Bullock, J., Kang, D., Phang, S.P., Weber, K., White, T., Macdonald, D., Catchpole, K., et al. (2023). Stability challenges for the commercialization of perovskite–silicon tandem solar cells. Nat. Rev. Mater. *8*, 261–281.

69. Fell, C.J. (2020). Standardising current–voltage measurements for metastable solar cells. J. Phys. Energy *2*, 11002.

70. Babics, M., De Bastiani, M., Ugur, E., Xu, L., Bristow, H., Toniolo, F., Raja, W., Subbiah, A.S., Liu, J., Torres Merino, L.V., et al. (2023). One-year outdoor operation of monolithic perovskite/silicon tandem solar cells. Cell Rep. Phys. Sci. *4*, 101280.

71. De Wolf, S., and Aydin, E. (2023). Tandems have the power. Science *381*, 30–31.

72. Chin, X.Y., Turkay, D., Steele, J.A., Tabean, S., Eswara, S., Mensi, M., Fiala, P., Wolff, C.M., Paracchino, A., Artuk, K., et al. (2023). Interface passivation for 31.25%-efficient perovskite/silicon tandem solar cells. Science *381*, 59–63.

73. Mariotti, S., Köhnen, E., Scheler, F., Sveinbjörnsson, K., Zimmermann, L., Piot, M., Yang, F., Li, B., Warby, J., Musiienko, A., et al. (2023). Interface engineering for high-performance, triple-halide perovskite–silicon tandem solar cells. Science *381*, 63–69.

74. Fischer A. Maxeon 40-year solar panel warranty available in select markets. PV Magazine USA; (2022). https://pv-magazine-usa.com/2022/02/04/maxeon-40-year-solar-panel-warranty-available-in-select-markets/. (accessed 2023-09-07).

75. Smith, K.D., Gummel, H.K., Bode, J.D., Cuttriss, D.B., Nielsen, R.J., and Rosenzweig, W. (1963). The solar cells and their mounting. Bell Syst. Tech. J. *42*, 1765–1816.

76. Macdonald, D., and Geerligs, L.J. (2004). Recombination activity of interstitial iron and other transition metal point defects in p- and n-type crystalline silicon. Appl. Phys. Lett. *85*, 4061–4063.

77. Yan, D., Cuevas, A., Stuckelberger, J., Wang, E., Phang, S.P., Kho, T.C., Michel, J.I., Macdonald, D., and Bullock, J. (2023). Silicon solar cells with passivating contacts: classification and performance. Prog. Photovolt. *31*, 310–326.

78. Chunduri S. High quality polysilicon, low RCZ content, no market for low grade wafers are key drivers for high costs associated with N-type wafers for HJT. Taiyang News; 2020. https://taiyangnews.info/technology/breakdown-of-higher-costs-n-type-wafers/. (accessed 2023-09-07).

79. Veirman, J., Varache, R., Albaric, M., Danel, A., Guo, B., Fu, N., and Wang, Y.C. (2021). Silicon wafers for industrial n-type SHJ solar cells: bulk quality requirements, large-scale availability and guidelines for future developments. Sol. Energy Mater. Sol. Cells *228*, 111128.

80. Basnet, R., Sun, C., Le, T., Yang, Z., Liu, A., Jin, Q., Wang, Y., and Macdonald, D. (2023). Investigating wafer quality in industrial Czochralski-grown gallium-doped p-type silicon ingots with melt recharging. Sol. RRL *7*, 2300304.

81. Vicari Stefani, B., Wright, M., Soeriyadi, A., Chen, D., Kim, M., Wright, B., Andronikov, D., Nyapshaev, I., Abolmasov, S., Wilson, G., et al. (2022). Silicon heterojunction solar cells and p-type crystalline silicon wafers: a historical perspective. Sol. RRL *6*, 2200449.

82. Taguchi, M. (2021). Review—development history of high efficiency silicon heterojunction solar cell: from discovery to practical use. ECS J. Solid State Sci. Technol. *10*, 25002.

83. Colville F. Which PV manufacturers will really drive n-type industry adoption? (2022). https://www.pv-tech.org/which-pv-manufacturers-will-really-drive-n-type-industry-adoption/. (accessed 2023-03-29).

84. Glunz, S.W., Rein, S., Knobloch, J., Wettling, W., and Abe, T. (1999). Comparison of boron- and gallium-doped p-type Czochralski silicon for photovoltaic application. Prog. Photovolt.: Res. Appl. *7*, 463–469.

85. Abe, T., Hirasawa, T., Tokunaga, K., Igarashi, T., and Yamaguchi, M. (2004). Silicon single crystal and wafer doped with gallium and method for producing them. US patent US6815605B1.

86. Richter, A., Müller, R., Benick, J., Feldmann, F., Steinhauser, B., Reichel, C., Fell, A., Bivour, M., Hermle, M., and Glunz, S.W. (2021). Design rules for high-efficiency both-sides-contacted silicon solar cells with balanced charge carrier transport and recombination losses. Nat. Energy *6*, 429–438.

87. Bivour, M., Schröer, S., Hermle, M., and Glunz, S.W. (2014). Silicon heterojunction rear emitter solar cells: less restrictions on

the optoelectrical properties of front side TCOs. Sol. Energy Mater. Sol. Cells *122*, 120–129.

88. Min, B., Wehmeier, N., Brendemuehl, T., Haase, F., Larionova, Y., Nasebandt, L., Schulte-Huxel, H., Peibst, R., and Brendel, R. (2021). 716 mV open-circuit voltage with fully screen-printed *p*-type back junction solar cells featuring an aluminum front grid and a passivating polysilicon on oxide contact at the rear side. Sol. RRL *5*, 2000703.

89. Min, B., Wehmeier, N., Brendemuehl, T., Merkle, A., Haase, F., Larionova, Y., David, L., Schulte-Huxel, H., Peibst, R., and Brendel, R. (2020). A 22.3% efficient p-type back junction solar cell with an Al-printed front-side grid and a passivating n^+-type polysilicon on oxide contact at the rear side. Sol. RRL *4*, 2000435.

90. Peibst, R. (2021). Still in the game. Nat. Energy *6*, 333–334.

91. Grant, N.E., Scowcroft, J.R., Pointon, A.I., Al-Amin, M., Altermatt, P.P., and Murphy, J.D. (2020). Lifetime instabilities in gallium doped monocrystalline PERC silicon solar cells. Sol. Energy Mater. Sol. Cells *206*, 110299.

92. Winter, M., Walter, D.C., and Schmidt, J. (2023). Impact of fast-firing conditions on light- and elevated-temperature-induced degradation (LeTID) in Ga-doped Cz–Si. IEEE J. Photovolt. *13*, 849–857.

93. Vicari Stefani, B., Kim, M., Wright, M., Soeriyadi, A., Andronikov, D., Nyapshaev, I., Abolmasov, S., Emtsev, K., Abramov, A., and Hallam, B. (2021). Stability study of silicon heterojunction solar cells fabricated with gallium- and boron-doped silicon wafers. Sol. RRL *5*, 2100406.

94. Danel, A., Chaugier, N., Veirman, J., Varache, R., Albaric, M., and Pihan, E. (2022). Closing the gap between n- and p-type silicon heterojunction solar cells: 24.47% efficiency on lightly doped Ga wafers. Published online October 21, 2022. Prog. Photovolt. 1–10.